ELSEVIER

Inorganica Chimica Acta 229 (1995) 171–178

Inorganica Chimica Acta

Atomic orbital energies in calcium to copper ☆

James L. Bills *, Richard L. Snow

Department of Chemistry, Brigham Young University, Provo, UT 84602, USA

Received 31 May 1994; revised 3 October 1994

Abstract

Three types of orbital energies, classified as ionizable, configurative, and additive, are found for Ca to Cu. The ionizable orbital energies explain the easier ionization of 4s than 3d in $M[Ar]4s^23d^N$. The configurative orbital energies select the ground configuration by approximating the Hartree–Fock energy of the transition $M[Ar]4s^23d^N \rightarrow M[Ar]4s^13d^{N+1}$. The additive orbital energies indicate the changes in the valence and core orbitals caused by the above transition. The changes in both the valence energy and the core energy are dominated by the change in valence exchange energy.

Keywords: Atomic orbital energies; Calcium; 3d Transition elements

1. Introduction

The connection between the ground-state electron configurations of the atoms Ca to Cu and the relative energies of their 4s and 3d orbitals has been elusive. One problem is that the orbital energies change whenever the configuration changes. Another problem is that the total energy of each configuration is not simply the sum of its orbital energies. A final problem is that the Hartree–Fock energy E_{HF} of each configuration is too high, because it does not provide adequate correlation between the probabilities of two electrons at various positions [1]. However, for the transition $M[Ar]4s^23d^N \rightarrow M[Ar]4s^13d^{N+1}$, ΔE_{HF} is fairly accurate (at least for Ca to Cr), because the correlation energies are similar in the two configurations [2].

In a study of average orbital energies, Claydon and Carlson (CC) noted that ϵ_{4s} is below ϵ_{3d} in K and Ca, and that ϵ_{3d} drops below ϵ_{4s} in Sc and beyond [3]. Griffin et al. studied the change in effective potential energy that is responsible for the sudden drop in ϵ_{3d} [4]. Evidently unaware of these studies, Pilar concluded that ϵ_{4s} is always above ϵ_{3d} in K and beyond [5].

Vanquickenborne, Pierloot, and Devoghel (VPD) solved for orbitals that are consistent with the weighted average of each configuration [6]. This average includes all terms with allowed values of spin S and angular momentum L. The ground term of each configuration, given by Hund's rules (highest S and highest L for that S), is surely of more interest to most chemists. One reason VPD gave for using the average is to be able to approximate the ionization energy of an electron i in an open subshell as $-\epsilon_i$ via Koopmans's theorem [7]. However, this can be done for the ground term simply by calculating ϵ_i for the spin-orbital that is vacated to give the ground term of the ionized configuration. We call such a spin-orbital and its energy ionizable. We shall find the ionizable ϵ_{4s} and ϵ_{3d} in the ground term of $M[Ar]4s^23d^N$ in Sc to Cu.

VPD showed that ϵ_{4s} and ϵ_{3d} have different values in $4s^23d^N$ than in $4s^13d^{N+1}$, and that a third value of ϵ_{3d} is found in $4s^03d^{N+2}$. They showed that the ground configuration cannot be determined by comparing these values of ϵ_{4s} and ϵ_{3d}.

VPD also used their average orbitals of $4s^13d^{N+1}$ to calculate the average energy of $4s^23d^N$. In that frozen-orbital approximation, the energy for the average of the transition $4s^23d^N \rightarrow 4s^13d^{N+1}$ is

$$\Delta E_{av1} = \epsilon_{3d}(4s^13d^{N+1}) - \epsilon_{4s}(4s^23d^N) \quad (1)$$

VPD found $\Delta E_{av1} < \Delta E_{avSCF}$, where ΔE_{avSCF} is the energy with self-consistent fields in both configurations. If VPD had frozen the orbitals of $4s^23d^N$ in the right-hand side of Eq. (1), they would have found $\Delta E_{av2} > \Delta E_{avSCF}$. With ΔE_{av1} too small and ΔE_{av2} too large, the average of the two should be about right. We shall pursue this approach for the transition between the ground terms of the two configurations in Ca to Cu.

☆ This paper is dedicated to Professor F.A. Cotton on the occasion of his 65th birthday.

* Corresponding author.

SSDI 0020-1693(94)04242-N

Blake studied the d–d Coulomb and exchange contributions to the ionization energy of $M^{2+}[Ar]3d^N$ [8]. The formulas that he lists for $d^N \rightarrow d^{N-1}$ are actually for $d^{N-1} \rightarrow d^N$. His ΔE_{rep} is the valence repulsion of the Nth d electron, whose ϵ is ionizable. In effect, Blake approximated this ionizable ϵ_{3d} as ΔE_{rep} with constant orbitals from Ti^{2+} to Zn^{2+}. Within this approximation, Blake showed that the drop in ionization energy at Fe^{2+} $3d^6$ is due more to the loss of exchange stabilization than to the extra Coulomb repulsion between two electrons in the same orbital.

Within Blake's approximation, his formulas and his conclusion also apply to the ionization of the Nth d electron from neutral $M[Ar]4s^23d^N$. We shall compare the ionizable ϵ_{3d} and the experimental 3d ionization energy with the valence exchange stabilization of the Nth d electron in neutral Sc to Cu.

The loss of exchange stabilization at d^6 that causes a drop in the d ionization energy at Fe and Fe^{2+} also causes a jump in the transition energy at Mn $4s^23d^5 \rightarrow 4s^13d^6$. CC concluded that exchange stabilization allows the 3d orbitals to shrink and thereby to exert greater repulsion on the 3s and 3p electrons, which in turn causes the 3s and 3p orbitals to expand. We shall examine the effect of the exchange energy on the core and valence energies.

VPD and CC both attempted to separate E_{HF} into Ar core and valence energies:

$$E_{HF} = E_c + E_v \quad (2)$$

The problem here is where to put the core–valence electron repulsions. VPD put them in E_v, while CC put them in E_c. Later, when CC chose to include as valence electrons all but the Ne core, they switched and put the core–valence repulsions in E_v.

There is no reason to assign the repulsion between two electrons i and j entirely to either i or j (unless it is done alternately to both, as in ϵ_i and ϵ_j). In this paper we present a meaningful way of assigning both i and j a portion of the repulsion between them. We use these additive electron repulsions to define additive orbital energies, which enable us to find meaningful values of E_c and E_v in Eq. (2).

2. Procedure

2.1. Orbitals

The orbitals in this work are for the ground terms of $M[Ar]4s^23d^N$ and $M[Ar]4s^13d^{N+1}$ in Ca to Cu. Most of the orbitals are due to Tatewaki and Sekiya (TS) [9,10]. The orbitals for $Ca[Ar]4s^13d^1$ are in Table 1. We kept most of the s and p basis functions of $Ca[Ar]4s^2$, but we optimized the d exponents, two p exponents, and all coefficients.

We also used the orbitals of $M[Ar]4s^23d^N$ in the configuration of $M[Ar]4s^13d^{N+1}$ and vice versa. When we used the $Ca[Ar]4s^2$ orbitals in the $Ca[Ar]4s^13d^1$ configuration, we used the 3d orbital from the $Ca[Ar]4s^13d^1$ orbitals. This procedure left Ca hardly comparable to the other atoms, but it sufficed.

All energies are in hartrees; 1 hartree $\approx$ 2625.56 kJ mol^{-1}.

2.2. Notation

Elaborating on VPD [5], we use the population of the 4s orbital to number the configurations, i.e., 1 for $4s^13d^{N+1}$ and 2 for $4s^23d^N$. Likewise, we number the orbital sets 1 and 2, where set 1 is self-consistent with $4s^13d^{N+1}$, and set 2 is self-consistent with $4s^23d^N$. The orbital set number is written first, followed by the configuration number as a superscript. Thus (1^2) means orbital set 1 in configuration 2, and (2^1) means orbital set 2 in configuration 1. Of course, only (1^1) and (2^2) are self-consistent.

Each neutral atom M has Z electrons. We assign the first $Z-1$ electrons to the ground term of $M^+[Ar]4s^13d^N$, so the Zth electron is the second 4s electron in $M[Ar]4s^23d^N$ and the $N+1$st 3d electron in $M[Ar]4s^13d^{N+1}$. We write the self-consistent orbital energies of electron Z as $\epsilon_{4sZ}(2^2) = \epsilon_{4s2}(2^2)$ and $\epsilon_{3dZ}(1^1) = \epsilon_{3dN+1}(1^1)$, with Z, 2, or $N+1$ on the same line as 4s and 3d. Likewise, we write the self-consistent orbital energies of the first 4s electron as $\epsilon_{4s1}(2^2)$ and $\epsilon_{4s1}(1^1)$. The average ϵ_{4s} of TS [9,10] for (1^1) is identical to our $\epsilon_{4s1}(1^1)$, but their ϵ_{4s} for (2^2) is the average of our $\epsilon_{4s1}(2^2)$ and $\epsilon_{4s2}(2^2)$. The ϵ_{3d} of TS for (2^2) is the average ϵ of the N 3d electrons, which we write as $\bar{\epsilon}_{3d}N(2^2)$, with the N above the line of 3d. In contrast, we write $\epsilon_{3dN}(2^2)$ for the Nth 3d electron in the aufbau sequence.

When both orbital sets are used to calculate a property in the same configuration, as in $\epsilon_{3dZ}(1^1)$ and $\epsilon_{3dZ}(2^1)$, the average of the two results is labeled with both set numbers, as in $\bar{\epsilon}_{3dZ}(12^1)$.

$$\bar{\epsilon}_{3dZ}(12^1) = [\epsilon_{3dZ}(1^1) + \epsilon_{3dZ}(2^1)]/2 \quad (3)$$

$$\bar{\epsilon}_{4sZ}(12^2) = [\epsilon_{4sZ}(1^2) + \epsilon_{4sZ}(2^2)]/2 \quad (4)$$

The *change* in any property in this paper is from configuration 2 to 1. If the change is from (2^2) to (1^1), the orbital sets and configurations are understood without being specified in the Δ of any property. For example, $\Delta E_{HF} = E_{HF}(1^1) - E_{HF}(2^2)$. If the orbital set is frozen, say at 1, we write $\Delta E_{HF}(1) = E_{HF}(1^1) - E_{HF}(1^2)$, for example. We define

$$\Delta\epsilon_Z(1) = \epsilon_{3dZ}(1^1) - \epsilon_{4sZ}(1^2) \quad (5)$$

and $\Delta\epsilon_Z(2)$ likewise. Notice that $\Delta E_{HF}(1) = \Delta\epsilon_Z(1)$ and $\Delta E_{HF}(2) = \Delta\epsilon_Z(2)$. We subtract Eq. (4) from Eq. (3) and find

Table 1
Orbitals of Ca[Ar]4s¹3d¹ ³D; total energy −676.67725 [a]

		1s	2s	3s	4s	
Energy ϵ		−149.27515	−16.71637	−2.14273	−0.19100[a]	
e		−192.10287	−31.86788	−6.08437	−0.40678	
n	Exponent	Coeff.				
1	29.61078	0.038241	−0.009595	0.005745	−0.001978	
1	19.42526	0.948530	−0.278221	0.090541	−0.018963	
2	18.21865	0.007826	−0.114114	0.053237	−0.014748	
2	10.82411	0.021225	0.418484	−0.178649	0.045844	
3	10.29046	−0.012484	0.286601	−0.045145	−0.002414	
3	8.01725	0.000503	0.446605	−0.334255	0.094252	
3	4.53259	−0.001755	0.029987	0.232406	−0.090035	
3	3.32037	0.001365	−0.012019	0.612083	−0.097686	
3	2.46463	−0.000541	0.004554	0.320845	−0.170358	
3	1.12200	0.000106	−0.000660	0.003640	0.300344	
3	0.75300	−0.000067	0.000412	−0.002017	0.770937	
3	0.45000	0.000017	−0.000102	0.000399	0.017093	

		2p	3p			3d
Energy ϵ		−13.52606	−1.25022			−0.12616
e		−31.00278	−4.84536			−1.07140
n	Exponent	Coeff.		n	Exponent	Coeff.
2	25.17785	0.002613	−0.000381	3	8.55000	0.013218
2	12.37123	0.164947	−0.055956	3	3.96000	0.145762
2	7.33368	0.782434	−0.160834	3	2.16600	0.296465
2	5.21639	−0.028594	−0.714725	3	1.09600	0.406716
2	4.74252	0.121528	0.439279	3	0.61600	0.392511
2	2.99163	−0.013900	0.172456			
2	2.13000	0.005365	0.874279			
2	1.40000	−0.000754	0.108196			

[a] For comparison, Ca[Ar]4s² has total $E = -676.75817$, 4s $\epsilon = -0.19553$ [10].

$$\Delta\bar{\epsilon}_Z(12) = \bar{\epsilon}_{3dZ}(12^1) - \bar{\epsilon}_{4sZ}(12^2) \quad (6a)$$

$$= [\Delta\epsilon_Z(1) + \Delta\epsilon_Z(2)]/2 \quad (6b)$$

$$= [\Delta E_{HF}(1) + \Delta E_{HF}(2)]/2 \quad (6c)$$

2.3. Experimental ionization and promotion energies

Experimental energies for the ground terms of $M[Ar]4s^23d^N$, $M[Ar]4s^13d^{N+1}$, $M^+[Ar]4s^13d^N$, and $M^+[Ar]4s^23d^{N-1}$ were taken from the works of Sugar with Corliss and Musgrove [11]. The term average was computed by weighting each J state by the factor $2J+1$. The energy ΔE_{exp} for the transition $M[Ar]4s^23d^N \rightarrow M[Ar]4s^13d^{N+1}$ is simply the difference between the term averages. Each of the ionization energies I_{4s2} and I_{3dN} of $M[Ar]4s^23d^N$ is the difference between the appropriate ion and atom term averages plus the ground-state ionization energy.

2.4. Additive interelectronic repulsions

Slater found a useful way to apportion the *charge* of each electron j that repels i [12(a)]. He set i at the radius r_i of its maximum charge density. He then apportioned the 1-charge of each other electron j into its inner screening, where $r_j < r_i$, and its outer screening, where $r_j > r_i$. He showed that the orbital exponent of i in level n_i is approximately Z_{fi}/n_i, where $Z_{fi} = Z - s_i$, and $-s_i$ is the total inner screening of i. Slater's screening constants are empirical rules for estimating s_i and hence Z_{fi} [12(b)]. See below for more about Z_{fi}.

We define $\overline{R}_{ji}$ to be the inner repulsion of i by j. The position of j inside i in $\overline{R}_{ji}$ symbolizes that $r_j < r_i$.

$$\overline{R}_{ji} = \int_{r_i=0}^{\infty} \int_{r_j=0}^{r_i} \sum_k a^k{}_{ij} P_i{}^2(r_i) P_j{}^2(r_j) r_j{}^k / r_i{}^{k+1} dr_j dr_i - \delta(m_{si}, m_{sj})$$

$$\times \int_{r_i=0}^{\infty} \int_{r_j=0}^{r_i} \sum_k b^k{}_{ij} P_i(r_i) P_j(r_i) P_i(r_j) P_j(r_j) r_j{}^k / r_i{}^{k+1} dr_j dr_i \quad (7)$$

In Eq. (7) $P_i(r_j) = r_j R_i(r_j)$, where $R_i(r_i)$ is the radial wave function of i for spherical coordinates [12(c)], and $a^k{}_{ij}$ and $b^k{}_{ij}$ stand for Slater's $a^k(\ell_i m_{si}; \ell_j m_{sj})$ and $b^k(\ell_i m_{si}; \ell_j m_{sj})$ [12(d)]. The subtotal repulsion of i is $\overline{R}_{ti}$:

$$\overline{R}_{ti} = \sum_{j \neq i} \overline{R}_{ji} \quad (8)$$

and the total interelectronic repulsion is the sum over i of $\bar{R}_{ii}$.

The second double integral in Eq. (7) is the inner exchange energy of i with j, $\bar{X}_{ji}$. We shall need the inner valence exchange energy of i,

$$\bar{X}_{vi} = \sum_{j \neq i}(v)\bar{X}_{ji} \tag{9}$$

and the total intervalence exchange energy

$$\bar{X}_{vv} = \sum_{i}(v)\bar{X}_{vi} \tag{10}$$

where v includes the 4s and 3d electrons. The total (inner+outer) valence exchange energy of i is $2\bar{X}_{vi}$.

Blake noted that $\bar{X}_{vv}$ (his ΣK) is often smaller with the cubic real d orbitals than with the imaginary orbitals indexed by m_ℓ [8]. We shall calculate $-2\bar{X}_{v3dN}(2^2)$ and $-\Delta\bar{X}_{vv}$ with both m_ℓ and cubic real orbitals.

2.5. Additive orbital energies

With additive interelectronic repulsions, the construction of additive orbital energies e_i is easy.

$$e_i = \bar{T}_i - \overline{Z/r}_i + \bar{R}_{ii} \tag{11a}$$

$$= \bar{T}_i + \bar{V}_{ii} \tag{11b}$$

where $\bar{V}_{ii} = -\overline{Z/r}_i + \bar{R}_{ii}$.

$$E_{HF} = \sum_i e_i = \sum_i \bar{T}_i + \sum_i \bar{V}_{ii} \tag{12a}$$

$$= \sum N_{n\ell}\bar{e}_{n\ell} \tag{12b}$$

where $N_{n\ell}$ is the number of electrons in the $n\ell$ subshell and $\bar{e}_{n\ell}$ is their average energy.

We use $\bar{e}_{3d}N(1^1)$ for the average e of the first N 3d electrons. We partition ΔE_{HF} for the $4s^23d^N \rightarrow 4s^13d^{N+1}$ transition via Eq. (2) as follows.

$$\Delta E_v = \Delta e_Z + \Delta e_{4s1} + N\Delta\bar{e}_{3d}N \tag{13}$$

$$\Delta E_c = 2\sum_{n=1}^{3}\Delta\bar{e}_{ns} + 6\sum_{n=2}^{3}\Delta\bar{e}_{np} \tag{14a}$$

$$= \Delta E_{Ne} + 2\Delta\bar{e}_{3s} + 6\Delta\bar{e}_{3p} \tag{14b}$$

ΔE_{Ne} is the change in energy of the neon core.

The simplest formula for ΔE_{HF} comes from Eq. (12b):

$$\Delta E_{HF} = \sum_{n\ell} N_{n\ell}(1^1)\bar{e}_{n\ell}(1^1) - \sum_{n\ell} N_{n\ell}(2^2)\bar{e}_{n\ell}(2^2) \tag{15}$$

We recommend Eq. (15), or its analogue for other systems, when there is no need to isolate Δe_Z. The subtotals ΔE_{Ne}, ΔE_c, and ΔE_v from Eq. (15) are identical to those from Eqs. (13) and (14). To adapt the data in Table 2 for Eq. (15), the following two equations are needed:

$$\bar{e}_{4s}(2^2) = \bar{e}_{4s}2(2^2) = [e_{4s1}(2^2) + e_{4s2}(2^2)]/2 \tag{16}$$

$$\bar{e}_{3d}(1^1) = \bar{e}_{3d}N + 1(1^1)$$

$$= [N\bar{e}_{3d}N(1^1) + e_{3dZ}(1^1)]/(N+1) \tag{17}$$

The virial theorem [12(e)] requires:

$$\sum_i \bar{V}_{ii} = -2\sum_i \bar{T}_i \tag{18}$$

When the left-hand side of Eq. (18) is substituted for the right-hand side and vice versa into Eq. (12a), we find

$$E_{HF} = \sum_i \bar{V}_{ii}/2 \tag{19}$$

$$E_{HF} = \sum_i -\bar{T}_i \tag{20}$$

Hence $\bar{V}_{ii}/2$ and $-\bar{T}_i$ are also additive orbital energies. In practice, the virial theorem is not satisfied perfectly, so Eqs. (19) and (20) are less accurate than Eq. (12). We compare values of $-\bar{V}_{ii}/2$ and $\bar{T}_i$ with those of $-e_i$ for Fe in Table 2.

Slater used his values of Z_{fi} to calculate approximate values of $\bar{T}_i$ for use in Eq. (20). In hartree units, his formula is

$$\bar{T}_i \approx (Z_{fi}/n_i)^2/2 \tag{21}$$

but for $n_i = 4$ he used $n^* = 3.7$ [12(b)].

3. Results and discussion

3.1. Ionizable orbital energies in $M[Ar]4s^23d^N$

The ionizable orbital energies $\epsilon_{4s2}(2^2)$ and $\epsilon_{3dN}(2^2)$ are compared with the corresponding ionization energies in Fig. 1. Koopmans's theorem correctly predicts easier ionization of 4s than 3d, but the experimental difference is smaller than expected from the orbital energies.

Fig. 1 also shows values of the valence exchange energy $-2\bar{X}_{v3dN}(2^2)$. These values are often smaller in magnitude with real orbitals than with m_ℓ orbitals, but the similarity is more striking than any difference. The net (Coulomb − exchange) repulsion in ϵ_{3dN} is the same for both real and m_ℓ orbitals. The correlation of ϵ_{3dN} and $-I_{3dN}$ with $-2\bar{X}_{v3dN}$ is obvious.

3.2. ΔE_{HF}, ΔE_{exp}, and $-\Delta\bar{X}_{vv}$ for $M[Ar]4s^23d^N \rightarrow M[Ar]4s^13d^{N+1}$

These values are shown in Fig. 2. Again, the correlation of ΔE_{HF} and ΔE_{exp} with $\Delta\bar{X}_{vv}$ is obvious. See also Fig. 3.

The values of ΔE_{HF} and ΔE_{exp} are also in Table 3. CC [3] attributed the difference between ΔE_{exp} and

Table 2
Additive orbital energies in M[Ar]4s²3d^N (top) and M[Ar]4s¹3d^{N+1}; values of $-e_i$ for Ca to Cu, and $-\overline{V}_{ii}/2$ and $\overline{T}_{n\ell}$ for Fe; top (2^2), bottom (1^1)

	$-\bar{e}_{1s}$	$-\bar{e}_{2s}$	$-\bar{e}_{2p}$	$-\bar{e}_{3s}$	$-\bar{e}_{3p}$	$-\bar{e}_{3d}$	$-e_{4sZ}$	$-e_{4s1}$	$-E$[Ar4s²3d^N]
Ca	192.0976	31.8540	30.9867	6.1605	4.9407		0.4849	0.4849	676.7582
Sc	212.1436	35.8640	35.0135	7.1889	5.8879	2.8338	0.5480	0.5524	759.7357
Ti	233.1908	40.1187	39.2872	8.2305	6.8436	3.6731	0.5936	0.6013	848.4060
V	255.2382	44.6142	43.8048	9.3104	7.8381	4.4729	0.6359	0.6467	942.8843
Cr	278.2859	49.3501	48.5652	10.4328	8.8761	5.2898	0.6759	0.6896	1043.3098
Mn	302.3339	54.3254	53.5685	11.5905	9.9494	6.1641	0.7111	0.7274	1149.8662
Fe	327.3806	59.5389	58.8127	12.8368	11.1180	6.9677	0.7637	0.7771	1262.4436
Fe [a]	326.5372	59.9049	58.8830	12.7200	11.0760	7.1294	0.7901	0.7969	1262.4412
Fe [b]	325.6937	60.2709	58.9533	12.6032	11.0340	7.2910	0.8166	0.8166	1262.4386
Fe [c]	330.24	59.68	59.68	12.09	12.09	2.17	0.51	0.51	1248.65
Co	353.4278	64.9913	64.2998	14.1195	12.3230	7.8526	0.8113	0.8214	1381.4145
Ni	380.4750	70.6821	70.0290	15.4497	13.5765	8.7878	0.8575	0.8643	1506.8709
Cu	408.5220	76.6114	76.0006	16.8286	14.8792	9.7710	0.9026	0.9060	1638.9500
	$-\bar{e}_{1s}$	$-\bar{e}_{2s}$	$-\bar{e}_{2p}$	$-\bar{e}_{3s}$	$-\bar{e}_{3p}$	$-\bar{e}_{3d}$N[d]	$-e_{3dZ}$	$-e_{4s1}$	$-E$[Ar4s3d^{N+1}]
Ca	192.1029	31.8679	31.0028	6.0844	4.8454		1.0714	0.4068	676.6772
Sc	212.1501	35.8810	35.0330	7.0840	5.7530	2.1608	2.1608	0.4312	759.6988
Ti	233.1975	40.1360	39.3071	8.1192	6.6996	2.9926	2.9853	0.4702	848.3861
V	255.2452	44.6321	43.8247	9.1939	7.6873	3.7916	3.7805	0.5103	942.8798
Cr	278.2932	49.3685	48.5860	10.3010	8.7074	4.6254	4.6254	0.5439	1043.3564
Mn	302.3402	54.3429	53.5878	11.4914	9.8210	5.4084	5.3281	0.5721	1149.7439
Fe	327.3877	59.5568	58.8329	12.7180	10.9690	6.2423	6.1969	0.5899	1262.3776
Fe [a]	326.5468	59.9162	58.8984	12.5792	10.9148	6.4005	6.3778	0.6333	1262.3771
Fe [b]	325.7058	60.2756	58.9638	12.4404	10.8606	6.5586	6.5586	0.6767	1262.3766
Fe [c]	330.24	59.68	59.68	12.09	12.09	1.93	1.93	0.39	1248.53
Co	353.4351	65.0093	64.3205	13.9923	12.1655	7.1251	7.0880	0.6053	1381.3584
Ni	380.4826	70.7008	70.0501	15.3154	13.4114	8.0521	8.0217	0.6188	1506.8240
Cu	408.5302	76.6302	76.0222	16.6793	14.6974	9.0341	9.0324	0.6270	1638.9637

[a] $-\overline{V}_{ii}/2$.
[b] $\overline{T}_{n\ell}$.
[c] $\overline{T}_{n\ell}$ from Eq. (21) via Slater's rules [12(b)].
[d] Each $\bar{e}_{3d}N$ is the average e of the first N 3d electrons.

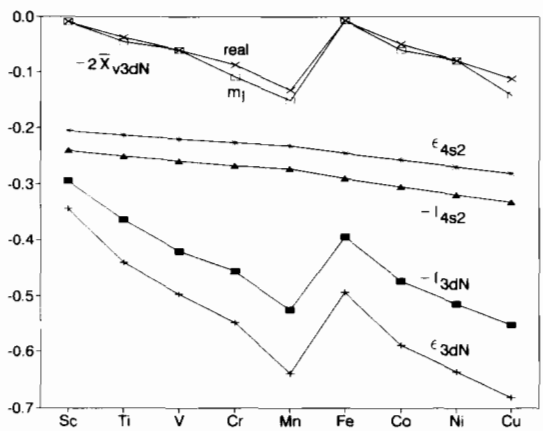

Fig. 1. Ionizable orbital energies, ionization energies [11], and the valence exchange energy of the Nth 3d for m_ℓ and cubic real orbitals (set 2) in M[Ar]4s²3d^N.

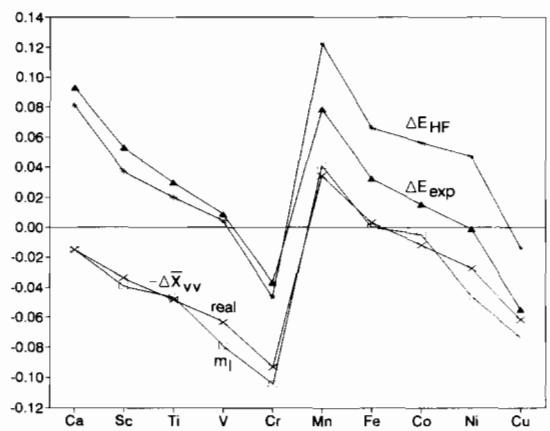

Fig. 2. Changes in the Hartree–Fock energy, the experimental energy [11], and the intervalence exchange energy for m_ℓ and cubic real orbitals in M[Ar]4s²3d^N → M[Ar]4s¹3d^{N+1}.

ΔE_{HF} mainly to the change in correlation energy. Their values of ΔE_{HF} can be obtained by subtracting their ΔE_{corr} from their ΔE_{exp}. Their values of ΔE_{HF} are higher than those in Table 3 by as much as 0.004 hartree.

3.3. Configurative orbital energies

The relationship between ionizable and configurative orbital energies is illustrated for Sc as follows:

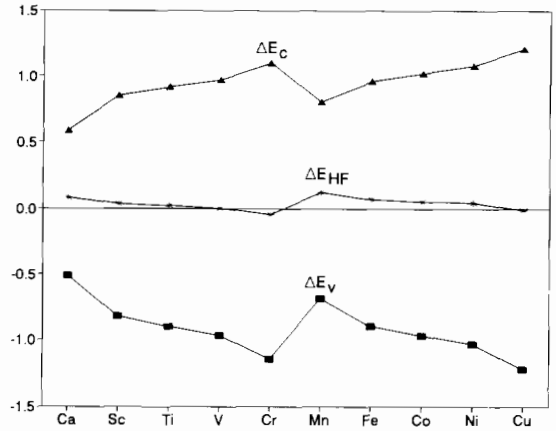

Fig. 3. Changes in the energies of the 4s+3d valence shell, the Ar core, and the Hartree–Fock atom in $M[Ar]4s^23d^N \rightarrow M[Ar]4s^13d^{N+1}$.

$\epsilon_{3dZ}(2^1)$		
$\uparrow\Delta\epsilon_Z(2)$	$\bar{\epsilon}_{3dZ}(12^1)$	
		$\epsilon_{4s1}(1^1)$
	$\uparrow\Delta\bar{\epsilon}_Z(12)$	
$\epsilon_{4sZ}(2^2)$		$\epsilon_{3dZ}(1^1)$
	$\bar{\epsilon}_{4sZ}(12^2)$	$\uparrow\Delta\epsilon_Z(1)$
		$\epsilon_{4sZ}(1^2)$
$\epsilon_{3d1}(2^2)$		
(22a)	(22b)	(22c)

In Sc, Z can be read as 2 in both ϵ_{4sZ} and ϵ_{3dZ}. The ionizable orbital energies are $\epsilon_{3d1}(2^2)$ and $\epsilon_{4sZ}(2^2)$ in Eq. (22a), and $\epsilon_{3dZ}(1^1)$ and $\epsilon_{4s1}(1^1)$ in Eq. (22c). In both of those pairs, we compare one electron in 4s versus a different electron in 3d.

In the aufbau process we want to compare the *same* electron Z in 4s versus 3d. This comparison is made in $\Delta\epsilon_Z(2)$, $\Delta\bar{\epsilon}_Z(12)$, and $\Delta\epsilon_Z(1)$. In Eq. (22a) $\Delta\epsilon_Z(2) = \Delta E_{HF}(2) > \Delta E_{HF}$ because $\epsilon_{3dZ}(2^1)$ is too high, since orbital set 2 is not consistent with configuration 1. In Eq. (22c) $\Delta\epsilon_Z(1) = \Delta E_{HF}(1) < \Delta E_{HF}$ because $\epsilon_{4sZ}(1^2)$ is too high, since orbital set 1 is not consistent with configuration 2. The average $\Delta\bar{\epsilon}_Z(12)$, given by Eq. (6) and shown in Eq. (22b), is close to ΔE_{HF} (see Table 3).

Fig. 4 shows the configurative orbital energies $\bar{\epsilon}_{4sZ}(12^2)$ and $\bar{\epsilon}_{3dZ}(12^1)$ from Ca to Cu. These curves are an improvement over those of Latter [13] that appear in textbooks [14]. Notice that in all of these atoms except Cr and Cu, $\bar{\epsilon}_{4sZ}(12^2)$ lies below $\bar{\epsilon}_{3dZ}(12^1)$. Hence the ground configuration selected by the configurative orbital energies is $M[Ar]4s^23d^N$ for all of these atoms except Cr and Cu, and $M[Ar]4s^13d^{N+1}$ for Cr and Cu.

The success of VPD [6] at finding a single set of orbitals for the average energy of a configuration suggests that a single set can be found with spin-orbital energies close to $\bar{\epsilon}_{4sZ}(12^2)$ and $\bar{\epsilon}_{3dZ}(12^1)$.

3.4. Additive orbital energies

Table 2 gives values of $-e_i$ for Ca to Cu, and for Fe values of $-\overline{V}_{ti}/2$, $\overline{T}_{n\ell}$, and $\overline{T}_{n\ell}$ from Eq. (21) via Slater's rules [12(b)]. Slater's rules work fairly well through the Ar core, but their estimate of $\overline{T}_{3d}$ is poor. Slater acknowledged that "the rules are far from quantitative..." [12(b)].

Slater noted that the force on an electron, and hence the form of its wave function that gives its kinetic energy, is determined by its inner shielding [12(a)]. By design, each e_i includes only the inner shielding, while its counterpart ϵ_i includes both inner and outer shielding.

In a given atom and configuration, the Hartree–Fock model uses the same orbitals, with the same $\overline{T}_{n\ell}$, for all electrons within a subshell. Then Eq. (11b) shows that any difference in e_i equals the difference in $\overline{V}_{ti}$. For example, Fe in Table 2 has $e_{3dZ}(1^1) - \bar{e}_{3d}N(1^1) = \overline{V}_{t3dZ}(1^1) - \overline{V}_{t3d}N(1^1)$.

Table 3
Configurative orbital energies and frozen-orbital approximations to ΔE_{HF} for $M[Ar]4s^23d^N \rightarrow M[Ar]4s^13d^{N+1}$ compared to ΔE_{HF} [9,10] and to ΔE_{exp} [11] (see Eqs. (3)–(6))

	$\Delta\epsilon_Z(2)$	$\Delta\epsilon_Z(1)$	$-\bar{\epsilon}_{4sZ}(12^2)$	$-\bar{\epsilon}_{3dZ}(12^1)$	$\Delta\bar{\epsilon}_Z(12)$	ΔE_{HF}	ΔE_{exp}
Ca [a]	0.0856	0.0748	0.1982	0.1180	0.0802	0.0809	0.0928
Sc	0.0867	0.0058	0.2135	0.1672	0.0463	0.0369	0.0524
Ti	0.0885	−0.0311	0.2228	0.1941	0.0287	0.0199	0.0296
V	0.0879	−0.0624	0.2308	0.2180	0.0127	0.0046	0.0090
Cr	0.0452	−0.1244	0.2376	0.2772	−0.0396	−0.0466	−0.0369
Mn	0.2511	0.0099	0.2454	0.1149	0.1305	0.1223	0.0788
Fe	0.1967	−0.0534	0.2601	0.1884	0.0716	0.0660	0.0322
Co	0.1967	−0.0769	0.2737	0.2138	0.0599	0.0562	0.0153
Ni	0.1982	−0.1006	0.2866	0.2378	0.0488	0.0469	−0.0011
Cu	0.1445	−0.1723	0.2985	0.3124	−0.0139	−0.0137	−0.0548

[a] From the orbitals in Table 1 and Ref. [10].

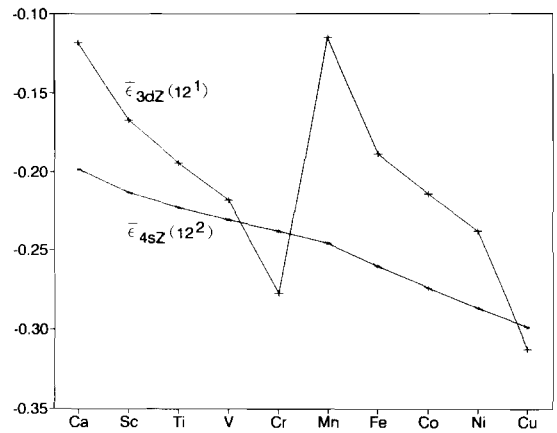

Fig. 4. The configurative orbital energy of electron Z in 4s2 of M[Ar]4s^{2}3d^N and in 3dN+1 of M[Ar]4s^{1}3d^{N+1}, each averaged over orbital sets 1 and 2.

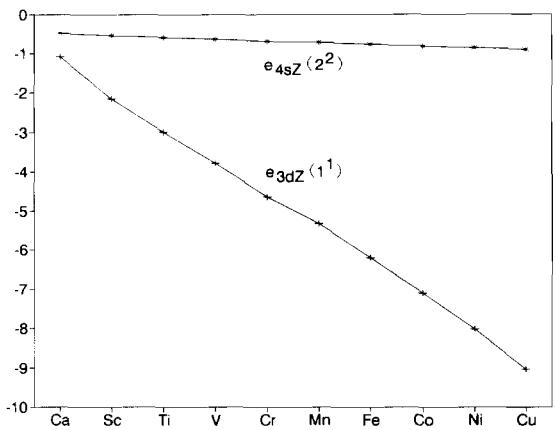

Fig. 5. The additive orbital energy of electron Z in 4s2 of M[Ar]4s^{2}3d^N and in 3dN+1 of M[Ar]4s^{1}3d^{N+1}.

To compare electrons in different subshells, it is best to use their average values $\bar{e}_{n\ell}$. The relative values of $\overline{V}_{tn\ell}/2$ and $-\overline{T}_{n\ell}$ are close to those of $\bar{e}_{n\ell}$. See how similar the values of $-\overline{V}_{tn\ell}/2$ and $\overline{T}_{n\ell}$ are to those of $-\bar{e}_{n\ell}$ for Fe in Table 2.

Since $\overline{V}_{tn\ell} \approx -\overline{Z_t/r}_{n\ell}$, the relative values of $-\bar{e}_{n\ell}$ also give a qualitative comparison of inverse size, $\overline{1/r}_{n\ell}$. Relative values of $\overline{V}_{tn\ell}/2$, $\overline{T}_{n\ell}$, and $\overline{1/r}_{n\ell}$ are indicated much better by $\bar{e}_{n\ell}$ than by $\bar{\epsilon}_{n\ell}$. For example, $\bar{\epsilon}_{3d}$ is slightly higher in V4s^{1}3d^4 (−0.3208) than in Sc4s^{2}3d^1 (−0.3437). Yet $\bar{e}_{3d}$ is much lower in V (−3.7888) than in Sc (−2.8338), indicating the correct order of $\overline{V}_{t3d}/2$ (−3.9217 versus −2.9545), $\overline{T}_{3d}$ (4.0545 versus 3.0752), and $\overline{1/r}_{n\ell}$ (0.9092 versus 0.7990) [9].

We recommend that $\bar{e}_{n\ell}$ be listed along with $\bar{\epsilon}_{n\ell}$ whenever atomic orbital energies are reported. The overbar can be dropped, as it was in Table 1.

Fig. 5 shows that $e_{3dZ}(1^1)$ lies below $e_{4sZ}(2^2)$. The transition 4s^{2}3d^N → 4s^{1}3d^{N+1} always has $\Delta e_Z < 0$, so it is never a *promotion* of electron Z in terms of e_Z. However, we shall see that the decrease in e_Z is often accompanied by a larger increase in the sum of the other e_i.

3.5. Components of ΔE_v and ΔE_c in M[Ar]4s^{2}3d^N → M[Ar]4s^{1}3d^{N+1}

The components of the changes in the valence and core energies in Eqs. (13) and (14b) are shown in Fig. 6. All of these changes can be rationalized as follows. When electron Z falls from 4s to 3d, its penetration of the 3s, 3p, and the other 4s and 3d electrons increases. From the frozen-orbital viewpoint of each other 4s or 3ℓ electron i, its inner screening increases by $\Delta\overline{R}_{ti}(2) = \overline{R}_{3dZi}(2^1) - \overline{R}_{4sZi}(2^2)$. From Eq. (11a) its $\Delta e_i(2) = \Delta\overline{R}_{ti}(2)$. When its orbital is unfrozen, the orbital has too much inner screening to stay the same size, so it expands. However, when the 4s and 3ℓ orbitals expand, their penetration of the 1s, 2s and 2p electrons decreases. The 1s, 2s and 2p orbitals shrink slightly, as seen in their $\bar{e}_{n\ell}$ and confirmed in their $\overline{1/r}_{n\ell}$ [9].

In the above analysis for $n_i > 2$, the frozen $\Delta\overline{R}_{ti}(2)$ is the cause of the frozen $\Delta e_i(2)$ and the unfrozen Δe_i. However, the interplay among the unfrozen orbitals can make the unfrozen $\Delta\overline{R}_{ti}$ unrecognizable as a cause of $\Delta\bar{e}_i$. In fact, an inverse correlation exists between $\Delta\bar{e}_{3d}N$ and $\Delta\overline{R}_{3d}N$. Further analysis of $\Delta\bar{e}_{3d}N$ via Eq. (11a) shows that $\Delta\overline{T}_{3d} - \Delta\overline{Z/r}_{3d}$ has a maximum at Mn, but $\Delta\overline{R}_{t3d}N$ has a *minimum* at Mn, in spite of a maximum there in $-\Delta\overline{X}_{t3d}N$. Analysis of $\Delta\bar{e}_{3p}$ shows that $\Delta\overline{T}_{3p} - \Delta\overline{Z/r}_{3p}$ has a minimum at Mn, but $\Delta\overline{R}_{t3p}$ is nearly zero from Ca to Cu.

The negative slope of Δe_Z is slightly greater in magnitude than the positive slope of $N\,\Delta\bar{e}_{3d}N$, so their sum has a slight generally negative slope. That sum plus the small positive values and slope of Δe_{4s1} gives ΔE_v.

The trends in 6 $\Delta\bar{e}_{3p}$ are like those in 2 $\Delta\bar{e}_{3s}$, although per electron $\Delta\bar{e}_{3p} > \Delta\bar{e}_{3s}$. These trends determine those in ΔE_c, because ΔE_{Ne} is fairly constant.

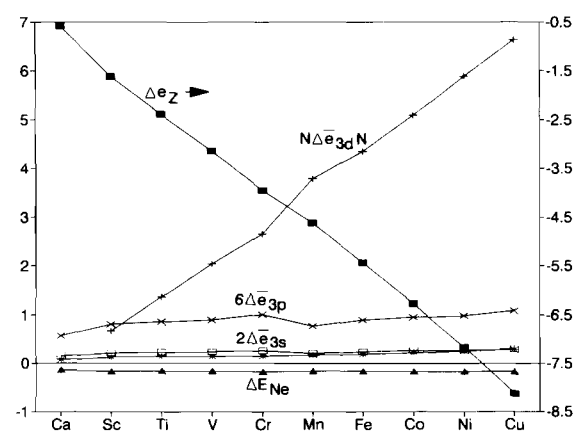

Fig. 6. Changes in the additive energies of the valence electrons Z, 3d^N, and 4s1, and of the Ar core electrons 3s^2, 3p^6, and Ne core in M[Ar]4s^{2}3d^N → M[Ar]4s^{1}3d^{N+1}. Each asterisk just below $2\Delta\bar{e}_{3s}$ is Δe_{4s1}.

3.6. ΔE_v and ΔE_c in M[Ar]4s²3d^N → M[Ar]4s¹3d^{N+1}

Fig. 3 shows the changes in the valence and core energies ΔE_v and ΔE_c, and their sum ΔE_{HF}(atom). ΔE_v looks a lot like $-\Delta\overline{X}_{vv}$ in Fig. 2, but on an amplified scale. ΔE_c shows a strong negative correlation with $-\Delta\overline{X}_{vv}$, also amplified. The dominant feature in all these plots is the jump from Cr to Mn. We divided each such jump in Fig. 3, e.g., $\Delta E_v(\mathrm{Mn}) - \Delta E_v(\mathrm{Cr})$, by $-\Delta\overline{X}_{vv}(\mathrm{Mn}) + \Delta\overline{X}_{vv}(\mathrm{Cr})$ to compute the factors by which $-\Delta\overline{X}_{vv}$ appears to be amplified in ΔE_v, ΔE_c, and ΔE_{HF}. With the m_ℓ orbitals, these factors are 3.2, −2.0, and nearly 1.2, respectively. With the real orbitals, the factors are even greater at 3.6, −2.3, and 1.3. In either case, the effects of $-\Delta\overline{X}_{vv}$ on ΔE_v, ΔE_c, and ΔE_{HF} are stunning.

4. Conclusions

The average valence orbital energies customarily given for M[Ar]4s²3d^N are not well suited to predict ionization energies or the energy of transition to M[Ar]4s¹3d^{N+1}. The ionizable valence orbital energies are $\epsilon_{4s2}(2^2)$ and $\epsilon_{3dN}(2^2)$. The ionization energy I_{3dN} and its estimate $-\epsilon_{3dN}(2^2)$ are strongly correlated with the valence exchange energy $2\overline{X}_{v3dN}(2^2)$. The configurative orbital energies $\bar{\epsilon}_{4s2}(12^2)$ and $\bar{\epsilon}_{3dN+1}(12^1)$ select the ground configuration by approximating ΔE_{HF} for M[Ar]4s²3d^N → M[Ar]4s¹3d^{N+1}.

Orbital energies e_i that include only the inner repulsion $\overline{R}_{ii}$ of other electrons are additive. The Hartree–Fock energy of any group of subshells such as core, valence shell, or atom is given simply by Eq. (12b). Each $\bar{e}_{n\ell}$ indicates $\overline{T}_{n\ell}$, $\overline{V}_{n\ell}/2$, and $\overline{1/r}_{n\ell}$ better than any ϵ does. For M[Ar]4s²3d^N → M[Ar]4s¹3d^{N+1}, Eqs. (13)–(15) give meaningful values of ΔE_v and ΔE_c as well as ΔE_{HF}(atom). The negative of the intervalence exchange energy $-\overline{X}_{vv}$ appears to be tripled in its stabilization of the valence energy and doubled in its destabilization of the core energy.

Acknowledgements

We thank the referees of an earlier manuscript for calling our attention to Ref. [6], and another referee for suggesting an improvement in notation.

References

[1] S.J. Chakravorty and E. Clementi, *Phys. Rev. A, 39* (1989) 2290, and references therein.
[2] C.W. Bauschlicher, Jr., S.P. Walch and H. Partridge, *J. Chem. Phys., 76* (1982) 1033.
[3] C.R. Claydon and K.D. Carlson, *J. Chem. Phys., 49* (1968) 1331.
[4] D.C. Griffin, K.L. Andrew and R.D. Cowan, *Phys. Rev., 177* (1969) 62.
[5] F.L. Pilar, *J. Chem. Educ., 55* (1978) 2.
[6] L.G. Vanquickenborne, K. Pierloot and D. Devoghel, *Inorg. Chem., 28* (1989) 1805.
[7] T.A. Koopmans, *Physica, 1* (1933) 104.
[8] A.B. Blake, *J. Chem. Educ., 58* (1981) 393.
[9] H. Tatewaki and M. Sekiya, *J. Chem. Phys., 85* (1986) 5895.
[10] M. Sekiya and H. Tatewaki, *Theor. Chim. Acta, 71* (1987) 149.
[11] (a) J. Sugar and C. Corliss, *J. Phys. Chem. Ref. Data, 14* (Suppl. 2) (1985); (b) J. Sugar and A. Musgrove, *J. Phys. Chem. Ref. Data, 19* (1990) 527.
[12] J.C. Slater, *Quantum Theory of Atomic Structure*, Vol. 1, McGraw-Hill, New York, 1960: (a) pp. 227–229; (b) pp. 368–372; (c) pp. 168–171; (d) p. 311; (e) p. 351.
[13] R. Latter, *Phys. Rev., 99* (1955) 510.
[14] F.A. Cotton and G. Wilkinson, *Advanced Inorganic Chemistry*, Wiley, New York, 5th edn., 1988, p. 628.